# Supplementary Information

## CHD7 cooperates with PBAF to control multipotent neural crest formation

**Ruchi Bajpai, Denise A. Chen, Alvaro Rada-Iglesias, Junmei Zhang, Yiqin Xiong, Jill Helms, Ching-Pin Chang, Yingming Zhao, Tomek Swigut and Joanna Wysocka**

**Content:**

**Supplementary Figures 1-13**

**Supplementary Tables 1-4**

## Supplementary Figure 1

**Migratory NCLC population is distinct from neural rosettes.**

The neuroectodermal origin of rosettes (white asterisks, panels a-c) was demonstrated by nuclear SOX2 immunostaining pattern (green, panel *c,* note nuclear localization in c")) and cytoplasmic NESTIN expression (red). Nuclear Sox2 localization, but not the filamentous distribution of NESTIN was lost in migratory hNCLCs (c). Inset c' highlights migratory hNCLCs and inset c" cells within a neural rosette, (*b*).

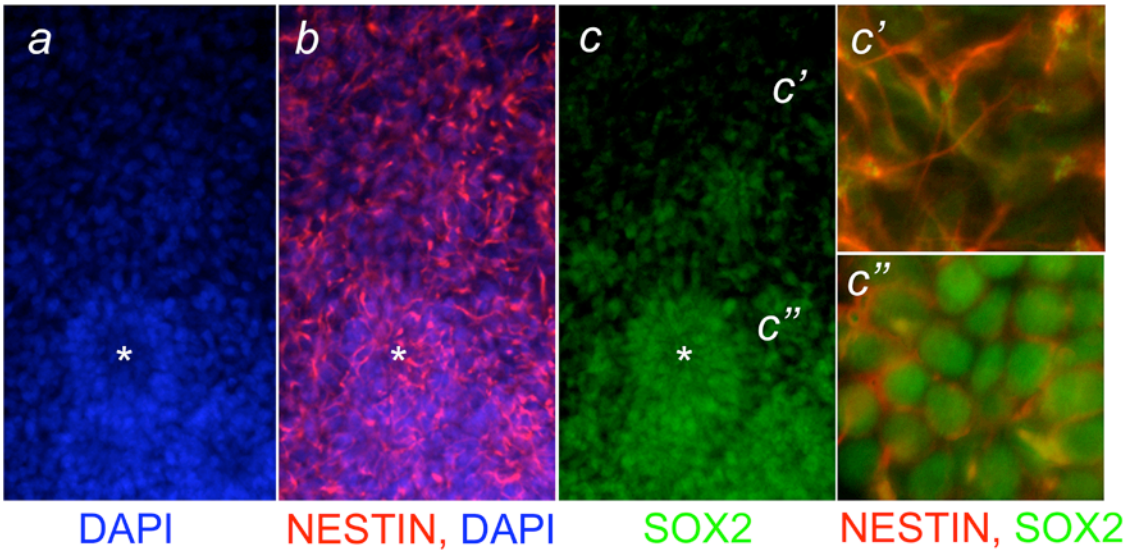

## Supplementary Figure 2

**hNCLC preferentially adhere to and proliferate on fibronectin-coated surfaces**.
Equal numbers of freshly derived hNCLC's were plated on tissue culture dishes coated with 5ug/ml fibronectin, or 10ug/ml laminin or 10 and 100 ug/ml poly L-ornithine. The cells attach and spread on fibronectin plates within 2hrs (not shown). At 12 hrs post plating, similar numbers of cells are attached in both fibronectin (a) and laminin (b) coated dishes. However, they fail to adhere to poly L-ornithine coated dishes (c). At the end of 48 hrs, significantly larger numbers of cells (>2.5 fold) are seen in fibronectin dishes when compared with the laminin coated ones, suggesting extra-cellular matrix components also influence proliferation rates of hNCLC.

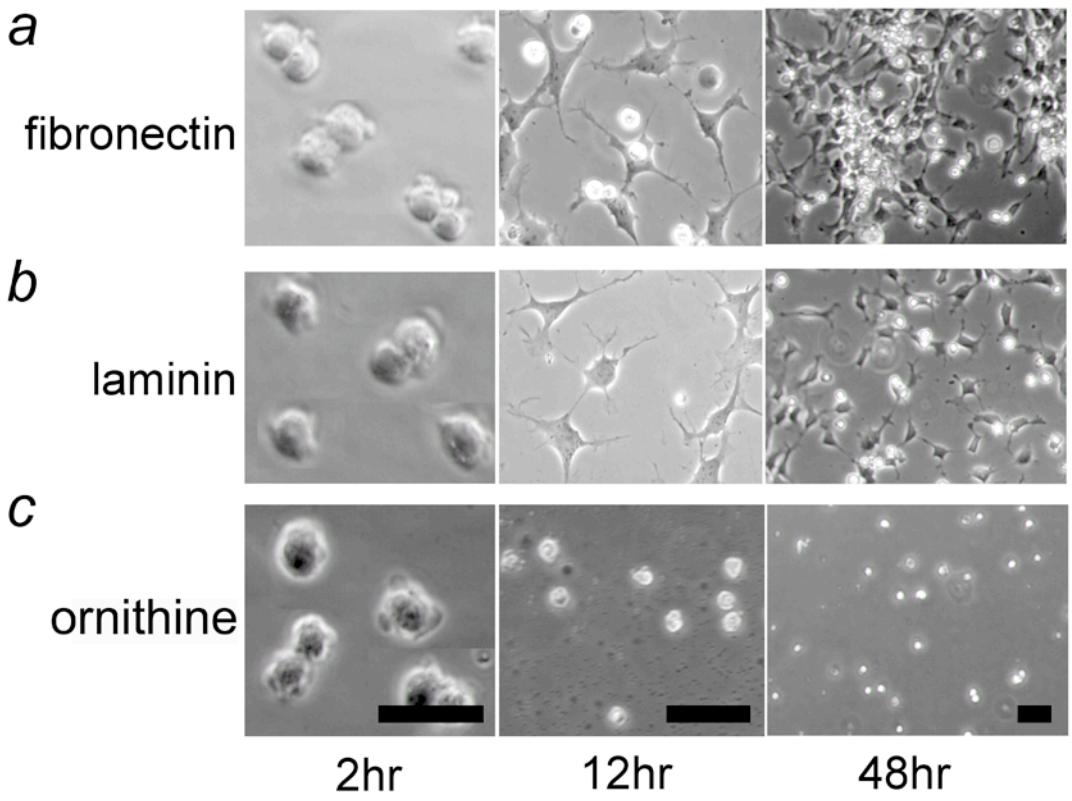

## Supplementary Figure 3

***In OVO* migration of hESC derived hNCLC.**

**(*A) Schematic representation of in OVO transplantation.*** Fluorescently labeled freshly migrated hNCLC were dissected with a needle as a cluster and without dispersal, transplanted into the developing neural tube of HH stages 8-10 chick embryos (dorsal view). The embryos were allowed to develop for 32 hrs and imaged between stages 14-20 (lateral view) (see methods for details).

(***B) and (C), Representative examples from two such experiments are shown.*** The labeled transplanted cells, imaged 6 hrs post transplantation (red arrows in a) shows precise localization to the neural tube. Within 32 hrs, the transplanted NCLC had migrated extensively from the neural tube (b). They were now detected within craniofacial mesenchyme( n= 4) and pharangeal arches( n=1+ 4) (white arrows in figs b) and also in the beating heart tube *in OVO* (n=1+2).

(***D) Floating spheres don't migrate.*** On the other hand, transplantation of the rosettes from unattached floating spheres primarily resulted in their integration within the neural tube (n=4), with very few if any migrating cells.

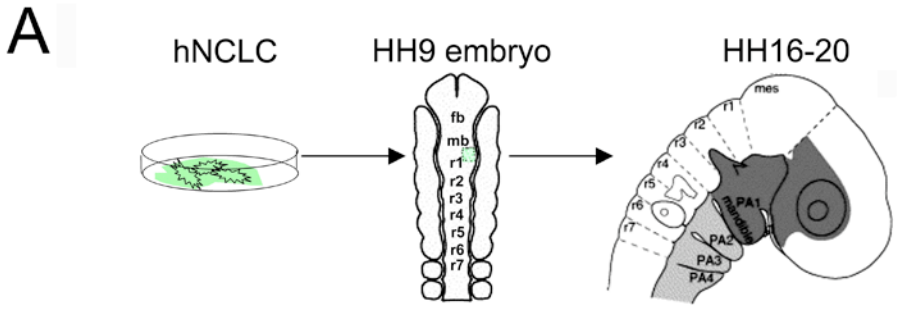
A
hNCLC
HH9 embryo
HH16-20
fb
mb
r1
r2
r3
r4
r5
r6
r7
mes
r1
r2
r3
r4
r5
r6
r7
PA1
mandible
PA2
PA3
PA4

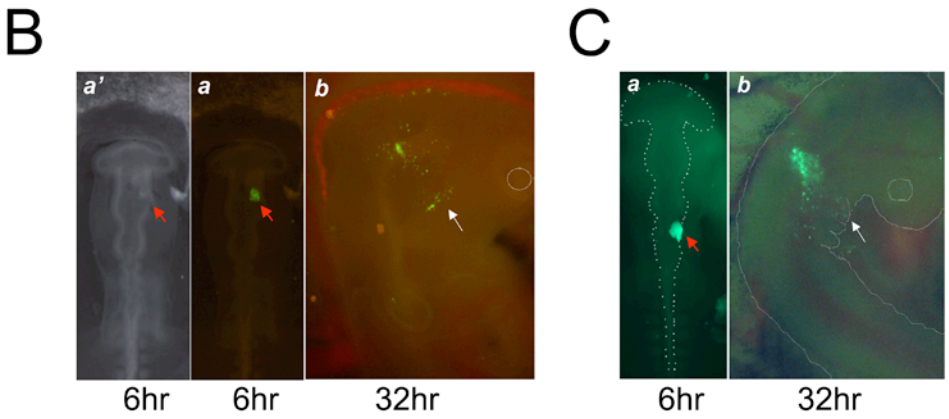
B
a'
a
b
6hr
6hr
32hr
C
a
b
6hr
32hr

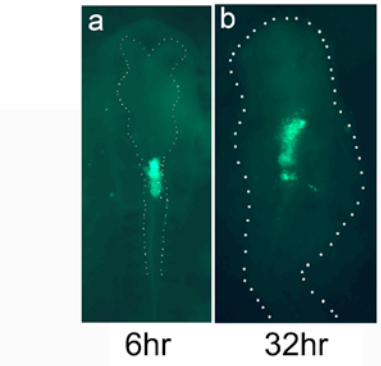
D
a
b
6hr
32hr

## Supplementary Figure 4

**hNCLCs derived from hESCs are multipotent.**

***(A) Schematic overview of the NCLC in vitro differentiation.*** hNCLCs newly derived from hESC can differentiate into multiple lineages upon growth factor withdrawal (*a*-*c*). Neuronal, melanocytic and mesenchymal derivatives were detected by immunostaining with neuronal markers being most abundant (>80% of the cells). In contrast, further amplification in the neural induction medium resulted in spontaneous maturation of hNCLCs into lineage-restricted precursors (*d*), which readily differentiate into mesenchymal cell types such as adipocytes and osteoblasts (*e*), but not neurons or glia, and are referred to as mesenchymal precursors (hMP).

***(B) Differentiation of hNCLCs to neural lineages.*** Expression of neural markers in differentiated hNCLCs was analyzed five weeks after induction of differentiation by immunostaining with antibodies recognizing: (*a*) an early neuronal marker bIII tubulin (also detected within a week of differentiation, not shown), (*b*) GFAP, a glial marker, (*c*) P2 myelin preferentially expressed in Schwann cells, and (*d*) peripherin, a type III intermediate filament preferentially expressed in mature motor neurons. As shown in *e*, several peripherin positive neuronal processes extended over 5mm in length. GFAP and peripherin were first detected after 4 weeks into differentiation.

***(C) Differentiation of hNCLCs to melanocytes and mesenchymal cell types.*** (a) MART1, a melanocyte marker, was reproducibly detected in compact cell clusters with similar numbers of melanin expressing pigmented cells. Adipocytes,osteoblasts and chondrocytes as assayed by Oil-Red O (*c*), alkaline phosphatase (*b* and *d*) and safranin O (*b*) staining, respectively, represented less than 5% of the differentiated cells.

Several attempts at cloning the NCLCs failed due to a high rate of cell death at clonal cell densities both in serum free and serum containing medium. However, the same cells, when plated at high density in neural induction medium, continued to proliferate without significant cell death and matured spontaneously into a morphologically distinct mesenchymal population (data not shown). Upon growth factor withdrawal these cells could no longer differentiate into neural lineages or melanocytes (confirmed by the absence of bIII tubulin, GFAP, MyelinP2 and MART1), but readily formed adipocytes (>85% cells) and osteoblasts (50-60% cells) under defined cell culture conditions.

A

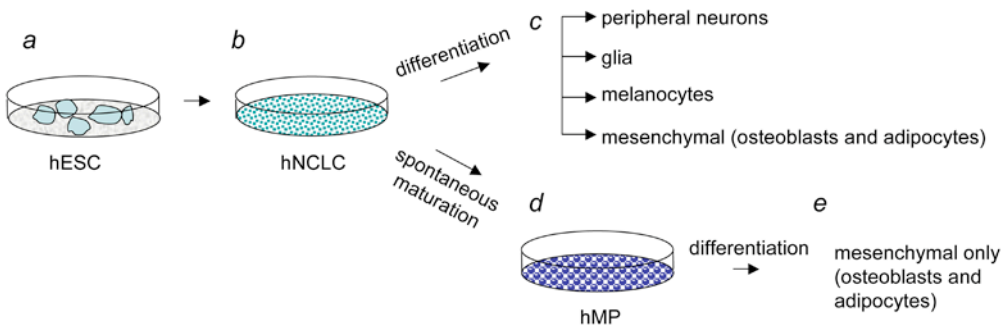
a
b
hESC
hNCLC
differentiation
spontaneous maturation
c
peripheral neurons
glia
melanocytes
mesenchymal (osteoblasts and adipocytes)
d
e
differentiation
mesenchymal only (osteoblasts and adipocytes)
hMP

B

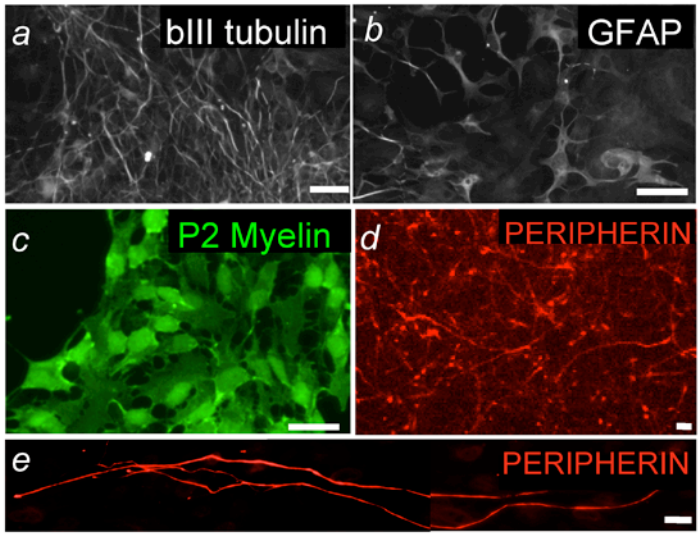
a
bIII tubulin
b
GFAP
c
P2 Myelin
d
PERIPHERIN
e
PERIPHERIN

C

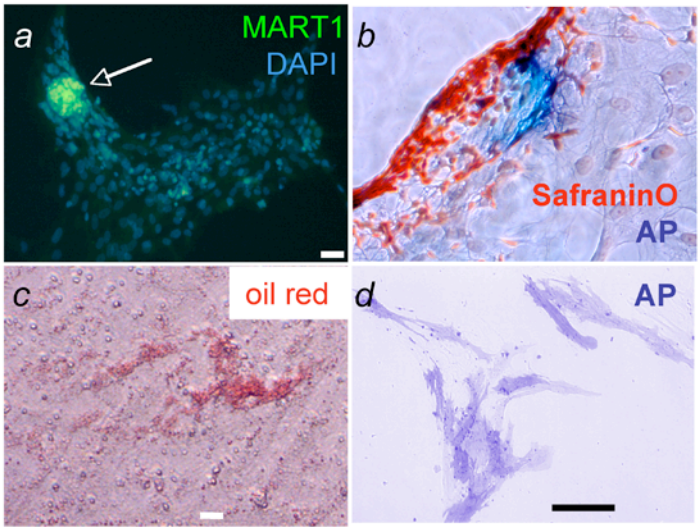
a
MART1
DAPI
b
SafraninO
AP
c
oil red
d
AP

## Supplementary Figure 5

**Inducible expression of CHD7 shRNA does not inhibit neural differentiation of hESCs.**

***(A) CHD7 mRNA expression levels.*** CHD7 mRNA expression levels were analyzed by quantitative RT PCR of RNA samples prepared from hESCs, hNCLCs and hMPs. Signals were normalized to SLC4A1AP, a housekeeping gene, whose expression fluctuates minimally during differentiation. Relative CHD7 expression is shown, with CHD7 expression in hESC normalized to 1 unit. Error bars represent the standard deviations from two independent biological replicate experiments.

***(B) Schematic representation of the Dox inducible lentiviral construct.*** The Ubiquitin C (UBC) promoter drives expression of reverse tetracycline transactivator 3 (rtTA3) along with puromycin resistance gene that was used for selection of transduced cells. In the presence of Dox, rtTA3 binds to TRE and activates the expression of a Turbo RFP and shRNAmir. The sequence shRNAmir used for human CHD7 RNA targeting is shown**.**

***(C) Dox inducible expression of shRNAmir.*** Differentiating hESCs, infected with either CHD7 shRNA (*a*-*d*) or the control shRNA (*e* and *f*) lentivirus emit red fluorescence in the presence (*d* and *f*) but not absence (*b*) of Dox. Top panels represent phase contrast and bottom panels red fluorescence channel.

***(D) CHD7 shRNA expression does not inhibit early neural differentiation of hESCs.*** CHD7 shRNA lentivirus infected cells form characteristic neural rosette structures (a) with neuronal processes (b and c).

***(E) CHD7 shRNA expression does not affect numbers of rosettes formed during differentiation.*** There is no significant difference between the number of spheres generated upon induction of differentiation from equally dense cultures of hESCs infected with CHD7 or control hairpin. The graph represents an spheres counted from two independent experiments.

A

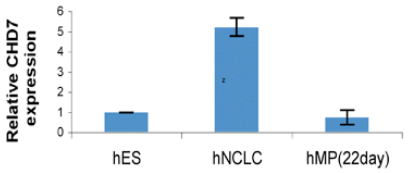


B

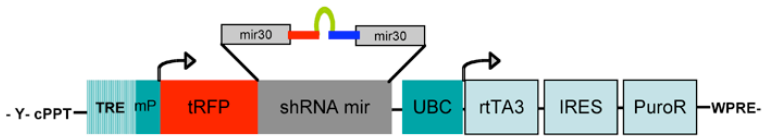


shCHD7 sense-loop-anti sense:
TGCTGTTGACAGTGAGCGAGGCAGTATTCTCGATATCCTT
TAGTGAAGCCACAGATGTA
AAGGATATCGAGAATACTGCCTACTGCCTCGGA

C

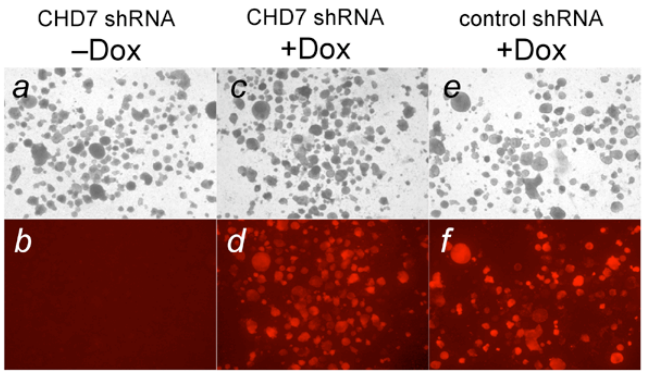


D

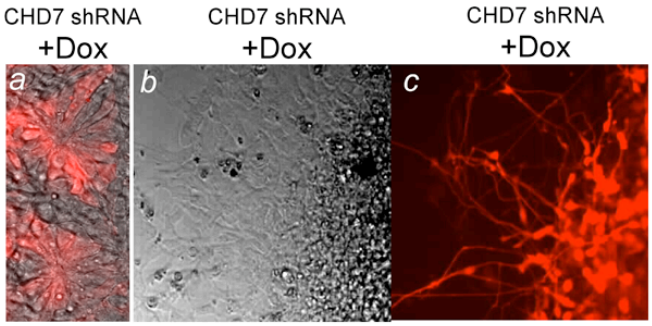


E

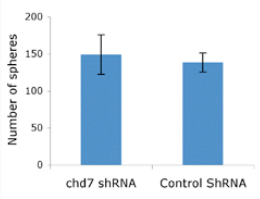

## Supplementary Figure 6

**A second CHD7 shRNA recapitulates defect in formation of hNCLCs.**

***(A) Schematic representation of the Dox inducible lentiviral construct encoding CHD7 shRNA2.***

***(B) Impaired migration from CHD7 shRNA2 expressing rosettes.*** hESC were infected with appropriate lentiviral shRNA vectors and induced to differentiate in the presence of Dox. At day 9 of differentiation, shRNA-expressing neural rosettes were identified by RFP expression at 10X magnification. Images contain merged fluorescence and bright-field.

***(C) PAX3 and TWIST1 expression in CHD7 shRNA-infected cells.*** hESCs were infected in parallel with CHD7 shRNA1 (described in the Supplementary Figure 5), CHD7 shRNA2 or control shRNAs and induced to differentiate in the presence of Dox. (***a***) Neuroectodermal cells (attached and floating rosettes) were collected as a single cell suspension and stained with α-PAX3 antibody. The number of PAX3/RFP double-positive and PAX3 positive/RFP negative cells was determined by cell counting (N >500) (***b***) In the same experiment, the hNCLCs were isolated by discarding the floating spheres and dissecting out the attached rosettes (>95% of isolated cells showed nuclear TWIST1 expression). The number of TWIST1/RFP double-positive and TWIST1 positive/RFP negative cells was determined by cell counting (N >500).

A

shCHD7-2 sense-loop-anti sense:
TGCTGTTGACAGTGAGCGACCAGTGGCTCACTTAACCAAA
TAGTGAAGCCACAGATGTA
TTTGGTTAAGTGAGCCACTGGTACTGCCTCGGA

B

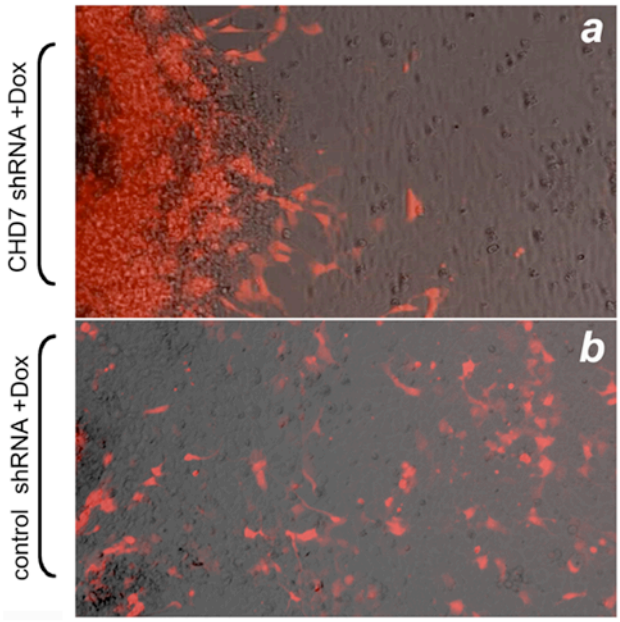


C

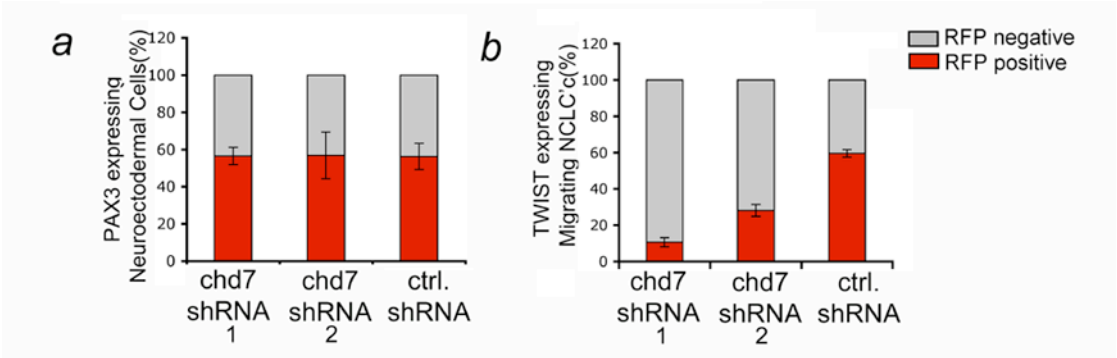

## Supplementary Figure 7

**Similarity between human and *Xenopus* CHD7.**

***(A) Conservation of domain architecture between Xenopus and human CHD7 proteins.***

A schematic representation of human and Xenopus CHD7 domain organization with amino acid identity over structural motif indicated. Note that the first 16 amino acids of the first chromodomain are only 11% identical, whereas remaining part is 90% identical between the two species.

(***B) Design of morpholino targeting both non-allelic forms of CHD7.*** Sequence of transcription start site region of two Xenopus leavis CHD7 genes (based on ESTs gi|12696661 and gi|24089657). The sequence targeted by the morpholino is underlined and the ATG codon shown in brackets.

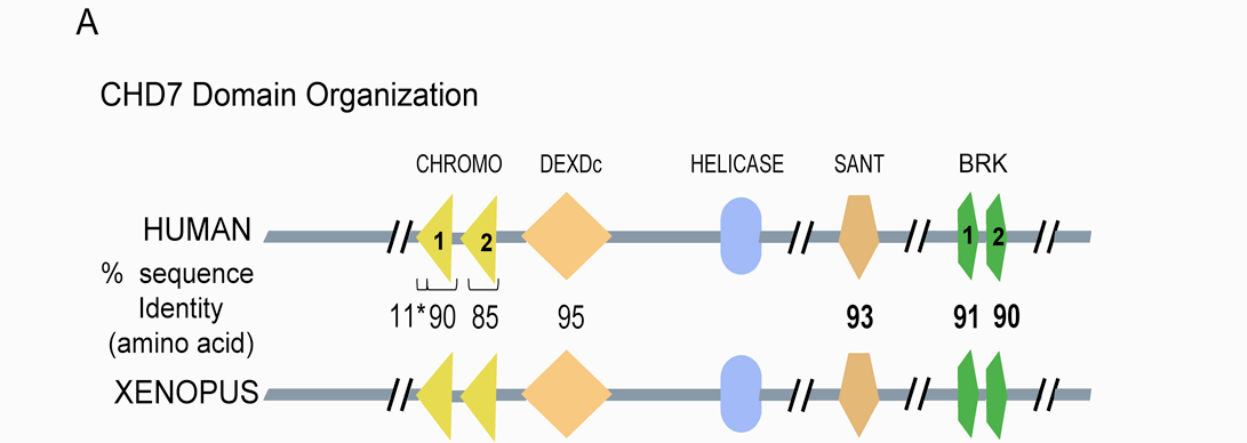

## Supplementary Figure 8

**Effects of CHD7 MO and hCHD7 ATP$^{K998R}$ overexpression on neural crest migration.**
***(A) Schematic of the neural crest migration assay in Xenopus laevis.*** Embryos were injected at the two-cell stage with mRNA encoding a photo-activatable protein Kaede with or without CHD7 morpholino oligonucleotide (CHD7 MO), or hCHD7 ATPK998R. At the neurula stage embryonic structures corresponding to a subset of the anterior neural and neural crest tissues were UV-irradiated to photo-convert Kaede protein from green to red fluorescence. Embryos were further developed to the tailbud stage to allow for visualization of neural crest cell migration to the pharyngeal arches (highlighted by arrows).
(***B) Quantification of the neural crest migration defect in CHD7 MO and hCHD7 ATP$^{K998R}$ injected embryos.*** Two-cell stage embryos were injected symmetrically into both blastomeres with Kaede mRNA and asymmetrically into a single blastomere with either CHD7 MO or hCHD7 ATP$^{K998R}$ and subsequently assayed for asymmetry in the cell migration pattern at the tailbud stage as described in A. The percentage of embryos exhibiting left-right asymmetry is indicated. Full or partial migration patterns are distinguished.
***(C) Defect in neural crest migration upon CHD7 knockdown in dorsal anterior structures and rescue with hCHD7 mRNA.*** CHD7 MO and/or hCHD7 mRNA was co-injected with a lineage tracer (mRNA encoding a fluorescent protein KikGR) into a single dorsal-animal (DA) blastomere of an eight cell stage embryo. The lineage label is clearly discernable along the pharyngeal arch tracts as well as parts of the neural tube and anterior head region (schematics). Injected embryos were subsequently scored for defects in the pharyngeal arch labeling pattern (we verified that all scored embryos were properly labeled in the neural tube and dorsal head regions). Full or partial migration patterns are distinguished. Co-injection of hCHD7 mRNA results in partial rescue of migration ($p<0.00042$; Fisher's exact test for count data).

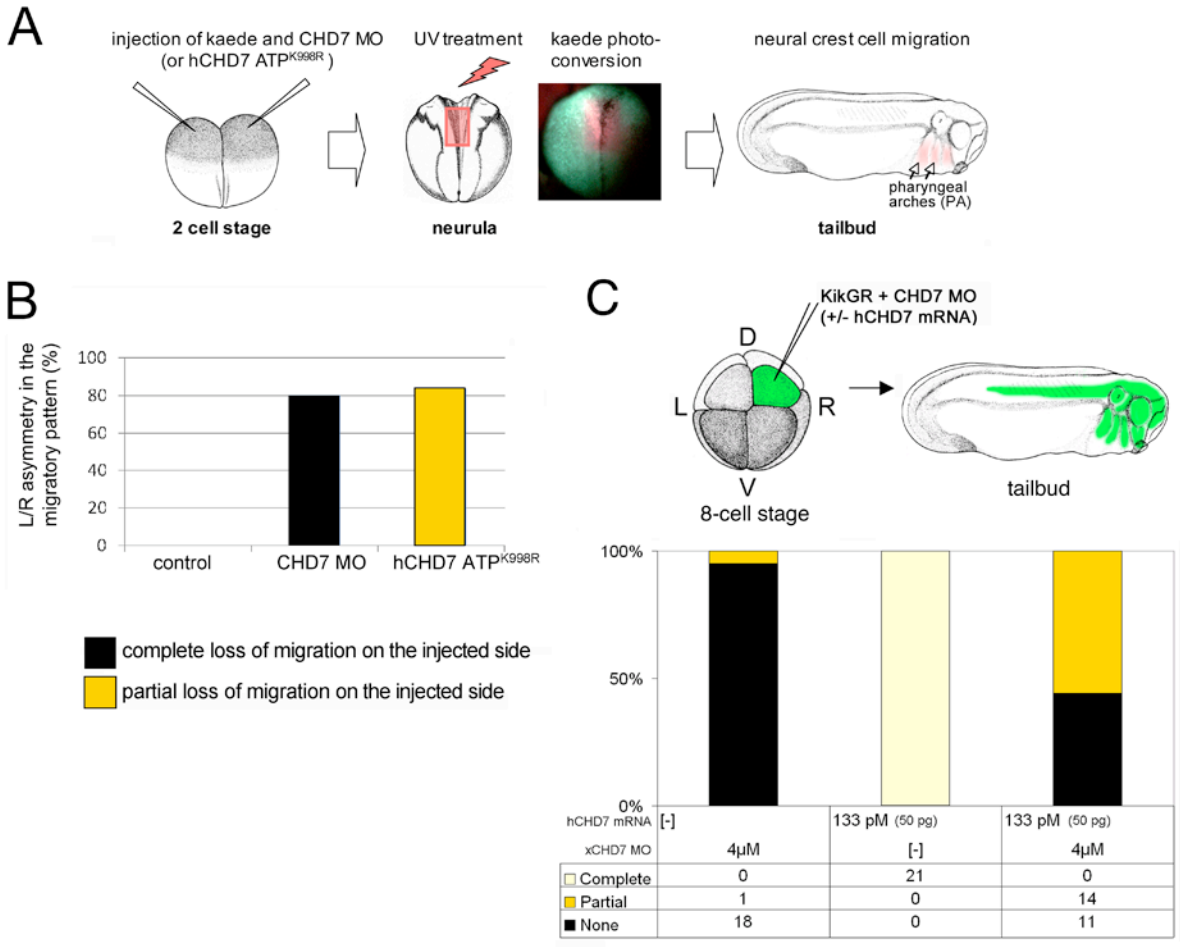


| hCHD7 mRNA | [-] | 133 pM (50 pg) | 133 pM (50 pg) |
|---|---|---|---|
| xCHD7 MO | 4μM | [-] | 4μM |
| Complete | 0 | 21 | 0 |
| Partial | 1 | 0 | 14 |
| None | 18 | 0 | 11 |

## Supplementary Figure 9

**Penetrance of craniofacial defects observed in *hCHD7 ATP$^{K998R}$* expressing tadpoles.**
***(A) Facial deformities resulting from overexpression of.*** Embryos at the two-cell stage were injected in both blastomeres with hCHD7 ATPase$^{K998R}$ and raised to the late tadpole stage for analysis. As compared to the uninjected control tadpoles (dorsal view in *a*, lateral view in *b*), embryos overexpressing hCHD7 ATPase$^{K998R}$ (*c-f*) exhibit anterior defects of varying penetrance, including as highlighted in orange on panels *e* and *f*, reduction of distance between the eyes (1), affected lens or retina (2), missing otolith(s) (3), frontal protrusion and facial flattening (4), and/or compression of the facial width (5).
***(B) Penetrance of anterior defects shown in A.*** The blue and red segments represent the percentage of scored tadpoles that do or do not, respectively, exhibit the indicated phenotypic trait. 25 tadpoles derived from eggs of three different females were scored for traits (1), (3), (5); 52 tadpoles derived from eggs 4 different females were scored for traits (2) and (4).

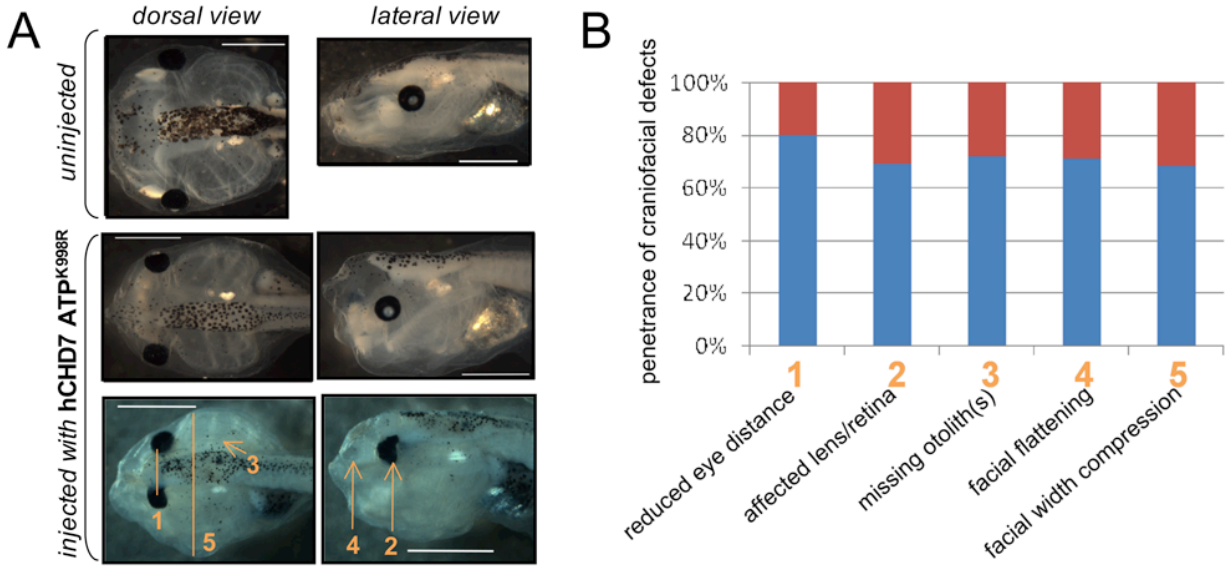

## Supplementary Figure 10

**Dosage-dependent effect of CHD7 MO.**

***(A) and (B) Kaplan-Meyer survival plots of two-cell staged embryos injected in both blastomeres with either CHD7 MO alone, CHD7 MO and hCHD7 mRNA, or human CHD7 mRNA alone***. Higher dosage of morpholino (5uM) was determined to cause embryonic lethality at the late neurula stage while a lower dose (3.3uM) of the morpholino caused partial lethality in addition to CHARGE like traits. Developing embryos were scored for viability on the y-axis at developmental stages indicated on the x-axis. Uninjected, as well as hCHD7 mRNA injected embryos exhibited 100% viability up to the stage 10.5.

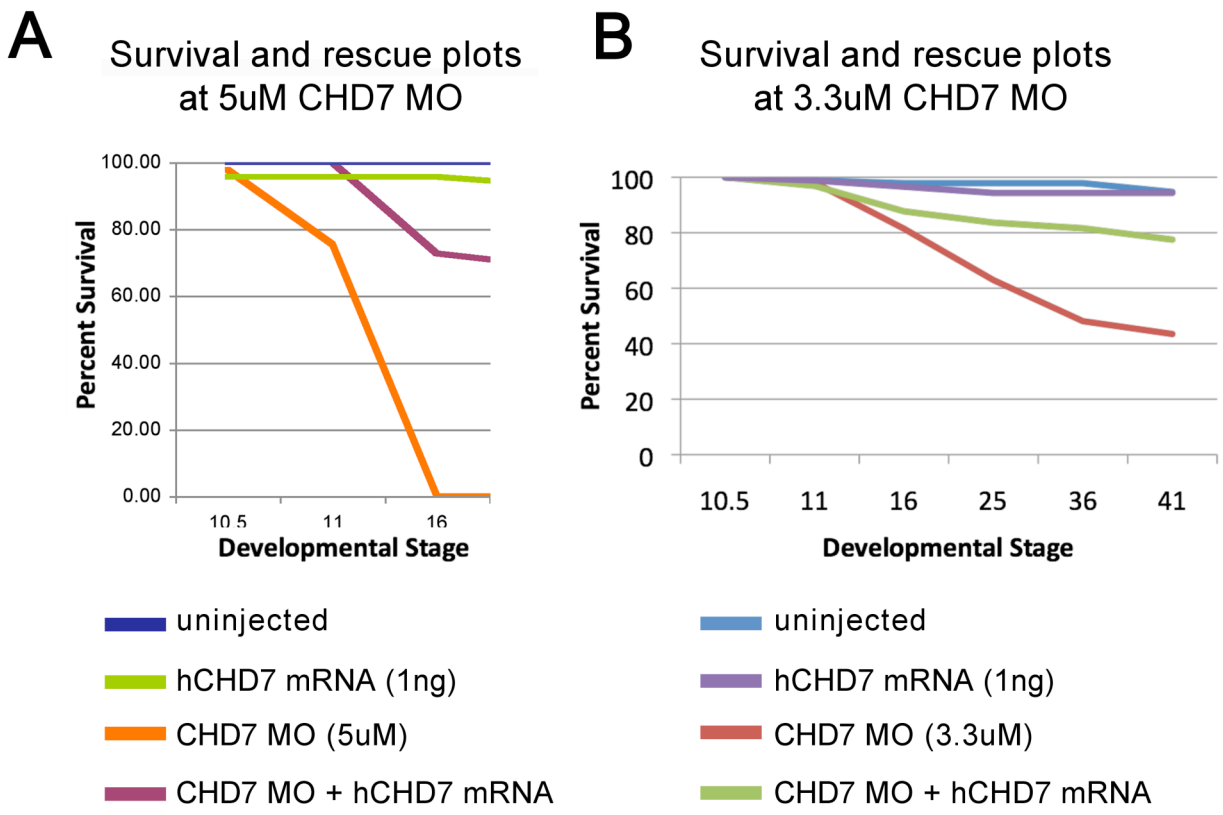

## Supplementary Figure 11

**Effect of CHD7 downregulation on Pax2 expression.**

Embryos were injected with CHD7 MO (3.3.uM) into a DA blastomere at the 8-cell stage with and allowed to develop to stage 22-24. Injected embryos along with uninjected controls were analyzed by RNA *in situ* hybridization for *Pax2* transcripts. Figure illustrates *Pax2* expression on the injected (top) and uninjected (bottom) side of the anterior region of a representative embryo. The spatial domains of *Pax2* expression shown are O: optic domain, OV: otic vesicle, BA: branchial arch, M-H: midbrain and hindbrain boundary. White arrows indicate the decrease in the intensity of *Pax2* staining in O, OV and BA in the injected side when compared to the analogous regions of uninjected control side (red arrows). M-H staining does not appear to be affected on the injected side ( n=7).

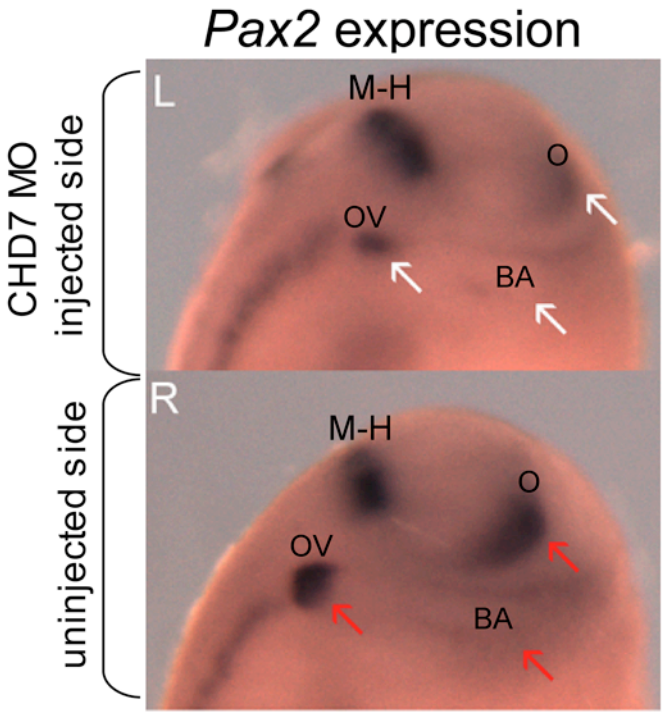

## Supplementary Figure 12

**Depletion of CHD7 from hNCLC nuclear extracts by a rabbit polyclonal antibody.** CHD7 or control antibody was used for immunoprecipitation from hNCLC nuclear extracts. Indicated fractions of total input, supernatant and immunoprecipitate were analyzed by immunoblotting with a different CHD7 antibody.

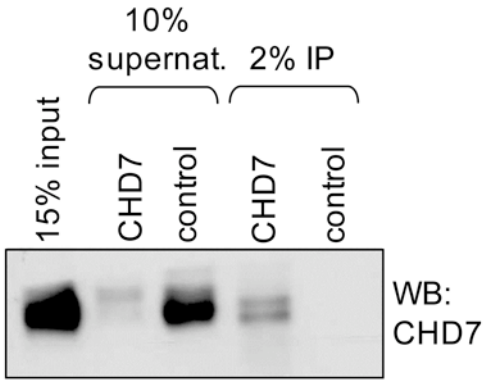

## Supplementary Figure 13

**Phenotypic overlap between embryos treated with morpholinos targeting BRD7 or BRG1 and CHD7 morphants.** Embryos were injected into DA blastomere at the 8 cell stage and raised to tadpole stages. The eye, otolith and anterior craniofacial features were imaged under a stereomicroscope. Representative images of age-matched CHD7, BRD7 and BRG1 morpholino injected embryos are shown.

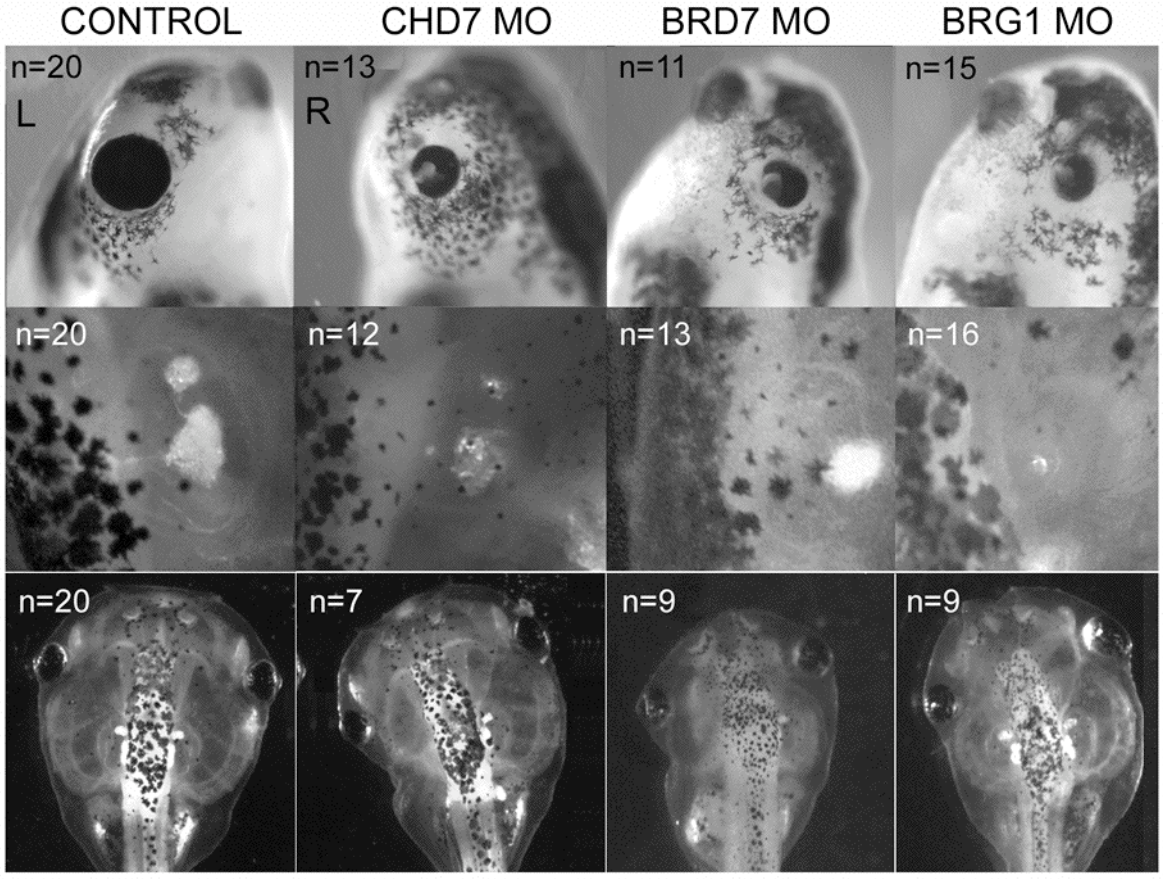

## Supplementary Table 1

### Summary of mass-spectrometry results

| | Accession # | Gene Name | Mascot Score NCLC | Mascot Score NT2 |
|---|---|---|---|---|
| | | | | |
| 1 | gi\|54112403 | chromodomain helicase DNA binding protein 7 | 10385 | |
| 2 | gi\|119607237 | chromodomain helicase DNA binding protein 7 | | 3041 |
| | | | | |
| 3 | gi\|1549241 | BAF 170 | 361 | 558 |
| 4 | gi\|10946129 | BRG1, SMARCA4 | 154 | 228 |
| 5 | gi\|21237802 | BAF 155, SMARCC1 | | 109 |
| 6 | gi\|133908629 | BAF 60a, SMARCAD1 | | 158 |
| 7 | gi\|119614672 | BAF 60b, SMARCAD2 | 56 | |
| 8 | gi\|21264353 | BAF 60c, SMARCAD3 | 48 | 309 |
| 9 | gi\|13937941 | BAF 57 | | 63 |
| 10 | gi\|440240 | BAF 47 | 78 | |
| | | | | |
| 11 | gi\|73921624 | BAF180, PB1 (Polybromo1) | 69 | 66 |
| 12 | gi\|41350212 | BRD7 (bromodomain containing 7) | | 58 |
| | | | | |
| 13 | gi\|156523968 | poly (ADP-ribose) polymerase family | 42 | 1246 |

## Supplementary Table 2

**List of antibodies used throughout the study.**

| | Antigen | Dilution Used | Company( catalog number) |
|---|---|---|---|
| Antibodies used for immunofluorescence and IHC | | | |
| 1 | AP2-a | 1 in 100 | Santa Cruz (sc-12726) |
| 2 | HNK1 | 1 in 1000 | Sigma (C 6680) |
| 3 | NESTIN | 1 in 500 | Chemicon (MAB 5326) |
| 4 | $P75^{NTR}$ | 1 in 200 | Promega (G323-A) |
| 5 | SOX2 | 1 in 300 | Chemicon (AB 5603) |
| 6 | SOX9 | 1 in 200 | Abcam (ab3697) |
| 7 | MART1 | 1 in 200 | Neomarkers; a kind gift from Barbara Bedougni |
| 8 | bIII TUBULIN | 1 in 500 | Covance(MMS-435P) |
| 9 | GFAP | 1 in 500 | Covance(SMI-22R) |
| 10 | P2 MYELIN | 1 in 500 | Santa Cruz (sc-49304) |
| 11 | PERIPHERIN | 1 in 500 | Chemicon (AB 1530) |
| 12 | DIGOXIGENIN | 1 in 1000 | Roche(AP conjugated Fab #11093274910) |
| Antibodies used for Western blotting | | | |
| 1 | CHD7 | 1 in 2000 | Abcam (ab31824) |
| 2 | CHD7 | 1 in 1000 | Bethyl Labs. ( A301-223) |
| 3 | xl CHD7 | 1:2000 | in house (see Methods) |
| 4 | Arid2 | 1:2000 | Abcam (ab51019) |
| 5 | BAF180(PB1) | 1:1000 | Bethyl labs (A301-591) |
| s6 | BAF170 | 1:1000 | Bethyl labs ( A301-038) |
| 7 | BAF155 | 1:1000 | (a kind gift from Dr. G. Crabtree) |
| 8 | BAF57 | 1:1000 | (a kind gift from Dr. G. Crabtree) |
| 9 | BRD7 | 1:2000 | Santa Cruz (sc101895) |
| 10 | BRG1 | 1:1000 | clone JA1 (a kind gift from Dr. G. Crabtree) |
| 11 | PARP1 | 1:2000 | Upstate (04-575) |
| 12 | RNApol11 | 1:4000 | Covance (MMS-126R) |
| Antibodies used for Immunoprecipitation/ ChIP | | | |
| 1 | CHD7 | 2-10ug | Abcam (ab31824) |
| 2 | PB1(BAF180) | 4ug | Bethyl labs (A301-591) |
| 3 | BAF170 | 4ug | Bethyl labs (A301-039) |
| 4 | BRG1 | 2-10ug | clone JA1 (a kind gift from Dr. G. Crabtree) |
| 5 | H3K4Me1 | 3ug | Abcam (ab 8895) |
| 6 | Mouse IgG | 2-10ug | MP Biomedical (55436) |
| 7 | RNApolII(8WG16) | 2-10ug | Covance (MMS-126R) |

## Supplementary Table 3

**List of RT-PCR and ChIP-qPCR primers.**

| Primer Name | Primer sequence (5' to 3') |
|---|---|
| **Primers used for RT- PCR** | |
| hCHD7-f | cttttcatgagccacaaacg |
| hCHD7-r | tcttcttcaaaagctttggtcac |
| hSLC4A1AP-f | gacactttgggattgcttcg |
| hSLC4A1AP-r | cccagttcttggctttcctt |
| **Primers used for ChIP-qPCR** | |
| Sox9 P1-f | TGGCAGTTTCAGTTGACCTTAG |
| Sox9 P1-r | GGCGTGTGCTTTGATTATAGG |
| Sox9 P2-f | TGGCAGTTTCAGTTGACCTTAG |
| Sox9 P2-r | GGCGTGTGCTTTGATTATAGG |
| Sox9 P3-f | GCAAGCTCTGGAGGTAGGAC |
| sox9 P3-r | GTTACACCCCATTCCCACTC |
| Twist P1-f | GCTAGAAGTTTAGTGCCGGG |
| Twist P1-r | GAGAAACCAAGTCCACAGCA |
| Twist P2-f | ACGACAGCCTGAGCAACA |
| Twist P2-r | ACAGCCCGCAGACTTCT |
| Control-f | CTCTTTGGCCATTCCTGATT |
| Control-r | GCCCAAGAGAGCGACTTTAC |

## Supplementary Table 4

**Primers used for Xenopus cDNA amplification.**

| Primer Name | Primer sequence (5' to 3') |
|---|---|
| MycII-f | cgtcggctcagcctgtggat |
| MycII-r | ctaacgggctgtggtgggct |
| Sox9-f | ttcattgagactgaggtgcgggaa |
| Sox9-r | tgtttagacatacaggcagggcca |
| Twist-f | ttctcatctgttgggacagagcct |
| Twist-r | taagtggcttcaaaggcacgactg |